RESEARCH ARTICLE

Drying of mushroom slices in a new type solar drying system and under open sun: Experimental and mathematical investigation

Kamil Neyfel Çerçi[1], Doğan Burak Saydam[2,3], Ertaç Hürdoğan[2,3*]

[1]Department of Mechanical Engineering, Engineering Faculty, Tarsus University, Tarsus, Türkiye.
[2]Department of Energy Systems Engineering, Engineering Faculty, Osmaniye Korkut Ata University, Osmaniye, Türkiye
[3] Energy Education-Etude Application and Research Center, Osmaniye Korkut Ata University, Osmaniye, Türkiye.

Orcid: K.N. Çerçi (0000-0002-3126-707X), D.B. Saydam (0000-0001-8453-2917), E. Hürdoğan (0000-0003-1054-9964)

Abstract: Drying is among the beneficial food preservation strategies and this method ensures food products last before they reach consumers. The most used drying method is direct drying under the sun. However, in this method, the negative effects of the external environment damage food products. Recently, solar drying systems have been the main subject of much research as they have been protecting food from the negative effects of the external environment. In this study, a solar drying system (SD), which have a drying chamber with different structure, was used for drying mushroom. At the same time, mushroom slices were dried under open sun (OSD) for observing the performance of drying system. Drying rate (DR) and moisture ratio (MR) values were determined from the experiments. In addition, the MR values obtained from the experiments were estimated by 6 different mathematical models and 6 different machine learning algorithms. According to the results of the experiments, the drying time of the mushroom slices using SD was approximately 12.4 hours less than the drying time under open sun. The best convergence in the results gathered from the mathematical models is Sripinyowanich and Noomhorn and Hii et al. models for SD and OSD, respectively. The best estimation for MR values was realized by the Multilayer Perception algorithm for both drying methods.

Keywords: Drying, Solar Energy, Open Sun, Machine Learning Algorithm, Thin-Layer Mathematical Modeling, Mushroom

1. Introduction

Drying is a popular food preservation method that decreases the moisture content of the product to an ideal level to avoid several types of deterioration, such as enzymatic and microbiological growth [1]. It is a heat and mass transfer process performed to extend the shelf life of fruits or vegetables that cannot be consumed during the drying season and to prevent product losses. Therefore, drying is an important activity in the food production chain [2]. In drying, the moisture content of the products is reduced, and thus, the product is protected. There are many methods such as direct sun drying, drying with solar energy assisted systems, heat pump drying, and microwave drying for drying foods [3-6]. Solar-assisted energy technology is an economical and clean energy source, and its usage is very popular in drying applications [7]. Solar dryers have two different modes of operation, passive (natural convection) and active (forced convection) [8]. In addition, solar drying systems can be used frequently in drying applications, as the product is protected against rain, dust, insects and animals during drying [9]. Turkey, located between 36°N and 42°N latitude, has a suitable

geographical location for solar energy. Turkey has an average yearly total sunlight length of 2640 hours (a daily total of 7.2 hours) and an average total irradiation of 1311 kWh/m²-year (a daily total of 3.6 kWh/m²) [10]. In this case, it increases the use of solar energy in many different applications, including drying applications [11-14]. Sun drying is the most prevalent way of preserving agricultural goods in most nations, including Turkey. However, this process is weather dependent and has issues with contamination with dust, dirt, and sand particles, drying time, time loss, and product loss [15]. Solar energy systems can be used easily in drying processes by having simple technology, low installation, and operating costs [16].

In the literature, there are many experimental and theoretical studies about solar energy-assisted drying systems. Aktas et al. [17] examined the drying of bay leaf in a closed-circuit heat-pump dryer. The researchers used ANN for modeling experimental data. Then, they evaluated the performance of the ANN model using indexes like the correlation coefficient (R^2), the root means square error (RMSE), and the mean absolute percentage error

(MAPE). The authors concluded that the predicted results were consistent with the experimental results. Doymaz [18] studied the influence of blanching and drying temperature on the drying kinetics and rehydration ratio of sweet potatoes and used several mathematical models to simulate the experimental data. It was shown that the logarithmic model has the best fit for experimental drying data. Kooli et al. [19] investigated the drying of red pepper under the sun and in the greenhouse and determined the drying time and moisture content of the products. The authors have developed a drying model to verify the drying pattern for MR. It was seen that the results obtained from the drying models were in good agreement with the experimental data. Chokphoemphun [20] conducted a numerical and experimental study on paddy drying in a rectangular fluid-bed dryer by applying the principle of swirling flow. In the experimental study, the author investigated the drying process for two different air inlet temperatures and two different air speeds in a drying time of 5 hours. The researcher calculated the predictive results of the experimental study as $R^2= 0,99556$, MSE= 1.988E-4 and MAE=0.00127. Süfer et al. [21] studied the drying of onions under different conditions. Authors examined the experimental data with 13 thin-layer drying models to select the model that best describes the relevant parameter. As a result of the study, the authors determined that the most suitable model among the drying models was the Sigmoid model. The Sigmoid model was followed by Cubic and Midilli models with respect to R^2, RMSE, and χ^2. As a result of the study, the authors determined that the diffusion coefficients ranged from 1.962×10^{-9} to 1.372×10^{-8} m²/s for convective, 9.757×10^{-9} and 1.723×10^{-8} m²/s for vacuum, and $3.193 10^{-8}$ to 9.139×10^{-7} m²/s for microwave drying.

In this study, the mushroom slices were dried with the open sun drying (OSD) method and solar dryer (SD) with a new type drying chamber in Osmaniye climatic conditions to obtain the of drying characteristics and to make a system comparison. Experimentally obtained MR values of dried mushroom slices were also estimated using 6 different thin-layer drying models and 6 different machine learning algorithms.

2. Materials and Methods

2.1. Experimental Setup

Representative scheme of the system [22,23] at the Osmaniye Korkut Ata University/Karacaoğlan Campus is appeared in Figure 1. The two basic pieces of equipment in the system are the drying chamber and the solar air collector. The system also includes a control panel, fan, and air duct for the circulation of the drying air. The ambient air (state 1) firstly enters the collector and then is transferred to the air inlet tunnel via a fan. Drying air whose temperature has increased inside the collector (state 2) removes the moisture from the products in drying chamber and is discharged into the outdoor environment (state 3). The drying chamber with an inclined structure was used to obtain homogeneous temperature distribution and to increase the drying performance. More detailed information about the drying channel and the system can be found in the other studies of the authors [22-24].

A glass wool insulating material was placed on the lower and side sides of the system's 195x95x12 cm (1.70 m²) plexiglass-cased air solar collector to help reduce the heat. A speed-controlled radial blower with a maximum flow rate of 650 m³/hr and a power output of 70W was employed to circulate the air. Silicon was used to seal all the connecting points and areas where air flows through in order to prevent air leaks. Additionally, a layer of glass wool
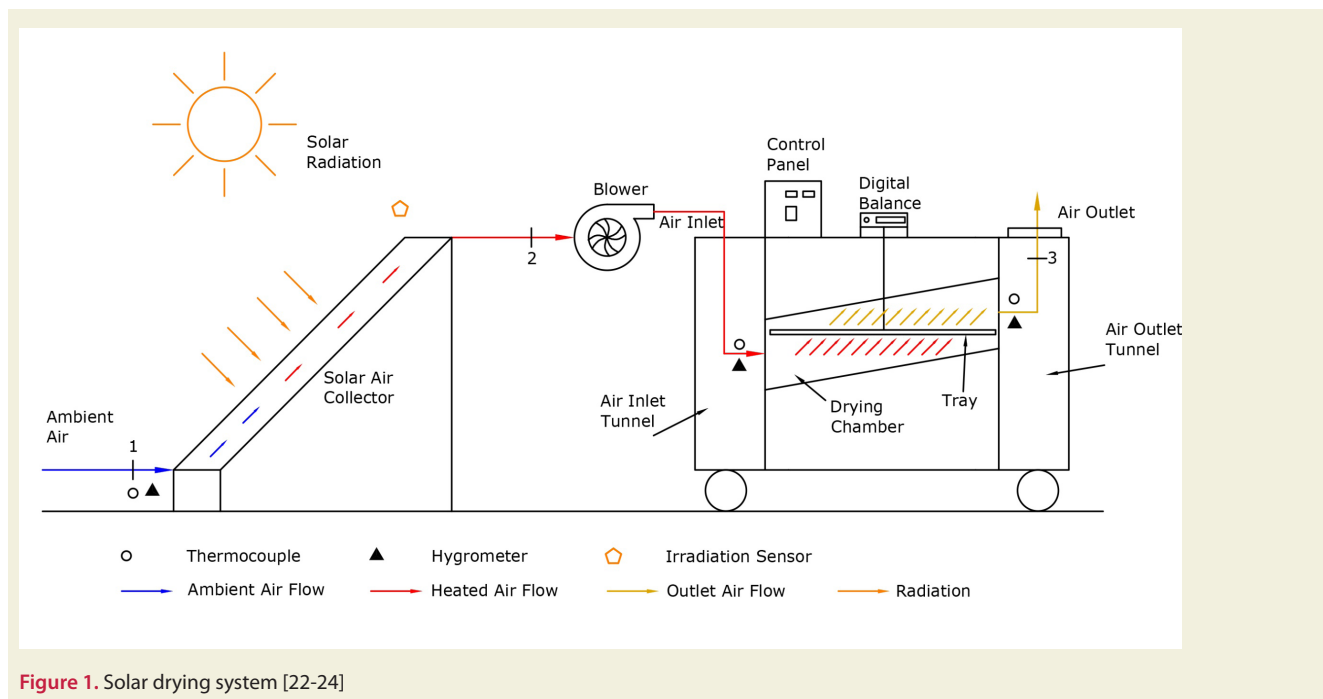

Figure 1. Solar drying system [22-24]

with an aluminum coating was placed atop the drying chamber to stop any potential heat losses. A transparent plastic sight glass is also included in the chamber for the purpose of monitoring the articles that need to be dried. Using a tray, the products that were to be dried were put inside drying chamber. To allow for air flow, a tray of roughly 0.5 m² was built of aluminium perforated wire. Following the product intake and introduction into the drying chamber, the tray is linked to the electronic scale by the chamber's hanger treatment (Figure 1-b).

2.2. Measurements and assessments of uncertainty

Measurements were taken at various stages (states 1-3) on the system (Figure 1) to assess the system's performance and the drying properties of the items to be dried. The temperature, relative humidity, and solar radiation were all measured by thermocouples, humidity transmitters, and irradiation sensors, in that order. The temperature measurements in the experiments were made with K type thermocouples. The air velocity measurement was carried out using an anemometer for defining the air mass flow rate. A computer-assisted data acquisition system was used to record the data within specified intervals. In the study, these measurement time intervals were determined as 15 minutes. The measurement equipment used for observing the performance of the experimental system is presented in Table 1. The most critical aspect influencing accuracy is mistakes that may occur throughout the trials for various reasons. The approach provided by Holman [25] was used for uncertainty (error) analysis. Uncertainty values of calculated parameter MR and DR are 2.30% and 2.60%, respectively.

Table 1. Measurement and analysis equipment

Device	Measurement parameters	Accuracy
TESTO 435 (Air Speed Probe)	Air velocity	0.1 m/s
COLE PARMER Thermocouple	Temperatures	0.1 °C
DİKOMSAN Electronic Balance	Product weight	0.1 g
EPLUSE Humidity Transmitter	Relative humidity	2-3 %
FRONIUS Irradiation sensor	Radiation	±5%
IOTECH PD3001 Data Logger	Data recording	16 bit

2.3. Thin-Layer Mathematical Modeling for Estimating MR

The quantity of moisture in food products is referred to as the product's water weight, and it is the most essential metric in drying procedures. Drying rate (DR, g_w / g_{dm}) and moisture ratio (MR) are used to determine drying behavior. DR is given in Equation 1 [26].

$$DR = \left(\frac{M_{t+dt} - M_t}{dt}\right) \quad (1)$$

MR is calculated using Equation 2 [22,24].

$$MR = \frac{M_t - M_e}{M_0 - M_e} \quad (2)$$

Here, M_t is defined as the amount of moisture at any time, M_0 is the amount of moisture at the beginning of drying, and M_e is called the equilibrium moisture amount of the product. The M_e value is too small for M_t and M_0. To simplify the computation of MR, M_t/M_0 is used instead of Equation 2 [26,27].

Mathematical, statistical, and numerical techniques are mostly used in drying processes to define the relationship among the different parameters of the system in the literature. In this study, the MR values gathered from the trials were estimated by different mathematical models. There are 6 mathematical models formed according to thin-layer drying used for modeling of MR and these models are presented in Table 2. Nonlinear regression analyses required to reveal the best model for defining the drying curve of the mushroom were carried out using the OriginPro 2017 software. The coefficient of correlation (R), the root mean squared error (RMSE) values were calculated to determine the convergence between MR obtained from experiments and from these equations.

The model with the highest R value and the lowest RMSE values obtained between the predicted results and experimental data was chosen as the best predicting model of MR values. The statistical values are calculated using the formula [21,26].

$$R = \frac{\sum_{i=1}^{n}(T_i - \bar{T})(P_i - \bar{P})}{\sum_{i=1}^{n}(T_i - \bar{T})^2 \sum_{i=1}^{n}(P_i - \bar{P})^2} \quad (3)$$

$$RMSE = \left[\frac{1}{N}\sum_{i=1}^{N}(MR_{pre,i} - MR_{exp,i})^2\right]^{\frac{1}{2}} \quad (4)$$

Ti and Pi are the neural network's target and predicted

Table 2. Methods used in modeling of MR

Model No	Model Constants	Formula	References
1	Hii et al.	y = a*exp (-k0*x^n) +b*exp (-k1*x^n)	[27]
2	Sigmoid	y = a + (b/(1+ exp(k*(x-c))))	[28]
3	Mod Midilli II	y = exp (-k*x) + b*x	[29]
4	Sripinyowanich and Noomhorn	y = exp (-k*x^n) + b*x + c	[30]
5	Noomhorn and Verma	y = a*exp (-k0*x) +b*exp (-k1*x) + c	[31]
6	Approximation of diffusion	y=(a*exp(-k*x))+((1-a)*exp(-k*b*x))	[32]

values; T and P are the neural network's average target and forecasted values; and n is total amount of input data. $MR_{exp,i}$ refers to the MR value obtained from the experimental observation, $MR_{pre,i}$ refers to the predicted MR value, N refers to the number of data obtained from observation, and n refers to the constants [21,26,33].

2.4. Machine Learning Algorithm for Estimating MR

Machine learning algorithms are divided into two classes as Unsupervised and Supervised Learning. The main element in supervised learning is the existence of a set of observations and the teaching of this training set to the system by a supervisor. As a result of this learning, it is necessary to make a prediction for a sample that has never been introduced before. As a consequence, the outcomes from the known data are used to develop the model for the solution. In this method, depending on the model developed, it is hoped to predict the results of data sets that lack label information. Most commonly used supervised learning algorithms can be listed as Multilayer Perceptron (MLP), Support Vector Machine (SVM) and M5P Tree (M5P), Random Forest (RF) [34].

In this study, MLP, SVM, RF and M5P algorithms were used to estimate the MR values obtained from the experiments carried out for drying of mushroom slices in SD and OSD. Input and output parameters used in machine learning algorithms for the predictive models are given in Table 3. These analyses were performed with Waikato Environment for Knowledge Analysis (WEKA) Version 3.8.3 software.

2.4.1. Support Vector Machine (SVM)

Support Vector Machines (SVM) is a classification method using structural risk minimization. The SVM was developed in 1995 by Cortesi and Vapnik for overcoming problems and increase the awareness of the unknown. The

foundations of SVM originate from the theory of statistical learning, which is called as Vapnik-Chervonenkis (VC) theory [35]. The general structure of SVM is displayed in Figure 2 [36].

SVM method, called Support Vector Regression (SVR), was created for estimating functions [37, 38]. SVR has the ability to capture a nonlinear relationship in property space. Therefore, it is accepted as an effective solution method for regression applications. [39]. In this study, PolyKernel (SVM_{Poly}) and NormalizedPolyKernel (SVM_{NPoly}) are used. The equations expressing SVM_{Poly} and SVM_{NPoly} kernel functions are given in Eq. 5 and Eq. 6, respectively [40].

$$K(x_i, y_i) = (x_i^T x_i + 1)^p \tag{5}$$

$$K(x_i, y_i) = \frac{(x_i^T x_i + 1)^p}{\sqrt{(x_i^T x)(x_j^T x_j)}} \tag{6}$$

2.4.2. M5P Tree

Quinlan [41], developed a new tree species, M5, to predict continuous variables. There is an important difference between the classification and regression tree (CART) and the M5 tree. The leaves of the regression trees created by CART have values. However, leaves of trees created by
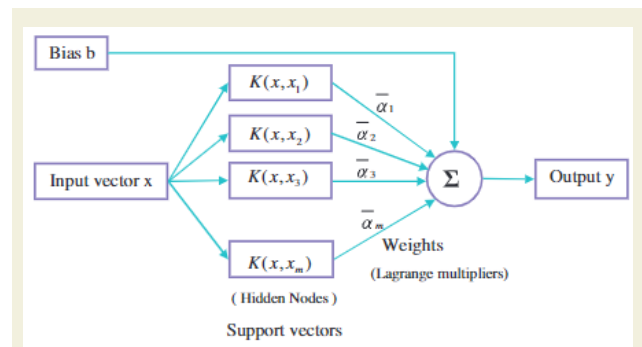

Figure 2. SVM's general structure [35]

Table 3. Input and output parameters

		Input		
Method	Parameter	Unit	Min	Max
SD	Drying Time [t]	Second	0	59400
	Radiation [I]	W/m²	0	795.27
	Ambient Temperature [T]	°C	16.43	28.65
	Ambient Relative Humidity [Rh]	%	21.75	51.81
OSD	Drying Time [t]	Second	0	103500
	Radiation [I]	W/m²	0	798.38
	Ambient Temperature [T]	°C	14.01	28.65
	Ambient Relative Humidity [Rh]	%	21.75	59.15
		Output		
Method	Parameter	Unit	Min	Max
SD	Moisture Ratio [MR]	-	0	1
OSD	Moisture Ratio [MR]	-	0	1

M5 have multivariate linear patterns. This feature offers the possibility of estimating the difference more flexibly. The M5 tree has three main steps. These include building trees, pruning trees, and smoothing trees. Standard deviation reduction (SDR), a parameter that the M5 tree seeks to maximize [42]. The equation of the SDR is presented below:

$$SDR = sd(T) = \sum_i \frac{|T_i|}{|T|} x sd(T_i) \tag{7}$$

here T is the set of states, Ti is the ith subset of states obtained via tree splitting using a set of variables, sd(T) is T's standard deviation, and sd (Ti) is Ti's standard deviation.

An expanded variant of the M5 algorithm is the M5P algorithm [43]. One of primary benefits of model trees is their ability to efficiently analyze huge quantities of datasets with many features and high dimensions. Also, they are able to overcome the missing data problems [44] powerfully. The SDR value defined in the M5P algorithm has been changed to take into account the missing values as follows [42]:

$$SDR = \frac{m}{|T|} x \beta_i x \left[sd(T) - \sum_{j \in \{L,R\}} \frac{|T_j|}{|T|} x sd(T_j) \right] \tag{8}$$

where T is the set of training examples for a node, β(i) is the correction factor for enumerated features, T_L and T_R are the split subsets, and m is the number of training cases with no missing values for an attribute.

2.4.3. Random Forest (RF)
Random Forest (RF) is a machine learning technique that is based on decision trees and was developed by Leo Breiman. A decision forest is formed by combining multiple decision trees and the estimation results obtained from each decision tree are combined to make a final estimate. Therefore, RF is a community learning method [34].

For each node in the work of Amit and Geman, Breiman combined the Bagging and the Random Subspace method, influenced by the output that the best distinction was determined by a random selection. First, the bootstrap technique forms a sample independent of the inputs. Then Random Subspace method selects a randomly selected number of variables from all variables and the best branching of each node [45].

2.4.4. Multilayer Perception (MLP)
The artificial neural network (ANN) is a modeling and estimation method that offers an alternative way of addressing complex problems and has a large-scale acceptance rate. Multilayer Perception (MLP) network feed forward is a type of neural network. The MLP networks are composed of an input layer, one or more hidden and output layers. Each layer has a number of units called neurons. These units are fully connected to the unit in the next layer with the weight relations. Therefore, the general expression of this network is as follows [45].

$$y = f_2 \left(\sum_{j=1}^{N} w_j f_1 \left(\sum_{i=1}^{n} h_{ij} X_i + b_j \right) + b_0 \right) \tag{9}$$

Here, y is predicted output, h_{ij}, b_j and f_1 are the weight matrix of the hidden layer, the bias factor of the hidden layer and the activation function of the hidden layer, respectively. w_j, b_0 and f_2 are the weight matrix of the output layer, the bias factor of the output layer and the activation function of the output layer, respectively [46].

Three layers make up the MLP model used in this investigation. Four neurons make up the input layer of the first layer. Eight neurons make up the second layer, sometimes known as the buried layer. The third layer, the output layer, is made up of one neuron. The hidden layer's activation function was determined to be the Sigmoid function. The learning rate was assumed to be 0.3. Figure 3 depicts the network structure.

3. Results and Discussions
In this study, through two days of experiments conducted in the Osmaniye climatic conditions, the drying properties of the mushroom slices were compared between open sun drying (OSD) and a solar collector-assisted drying system (SD). Before the experiment, contaminants such as dust and soil on the mushrooms were cleaned and products were cut into thin slices of almost the same size. The sliced products are arranged in a single row in trays to be used in the drying chamber and under the sun. The weight of the products placed on the tray was set to be approximately the same (1410 g). The drying process continued until the products reached equilibrium moisture. During the drying process, the measured parameters are incident radiation, product weight, temperature and relative humidity, respectively. As mentioned earlier, these measurements were performed at 15-minute intervals and
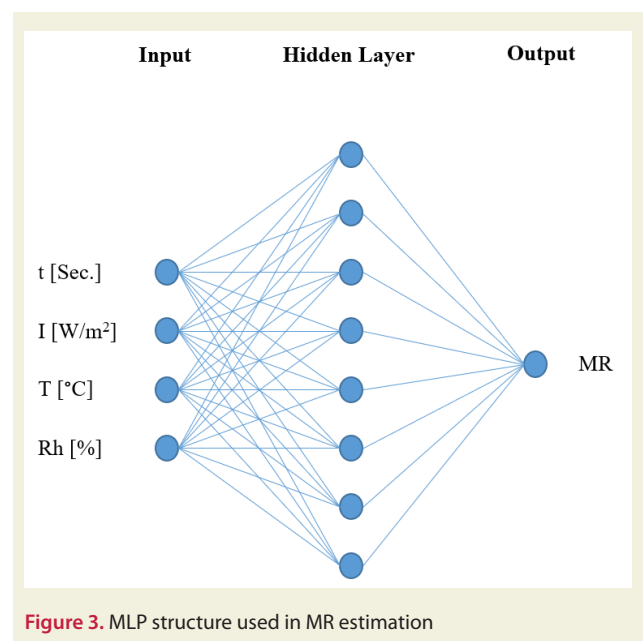

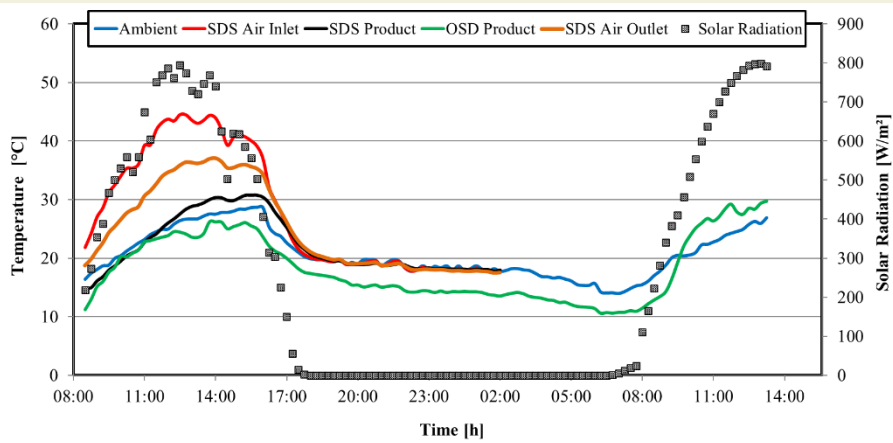**Figure 3.** MLP structure used in MR estimation

Figure 4. Variations of temperature and radiation during the drying of mushroom
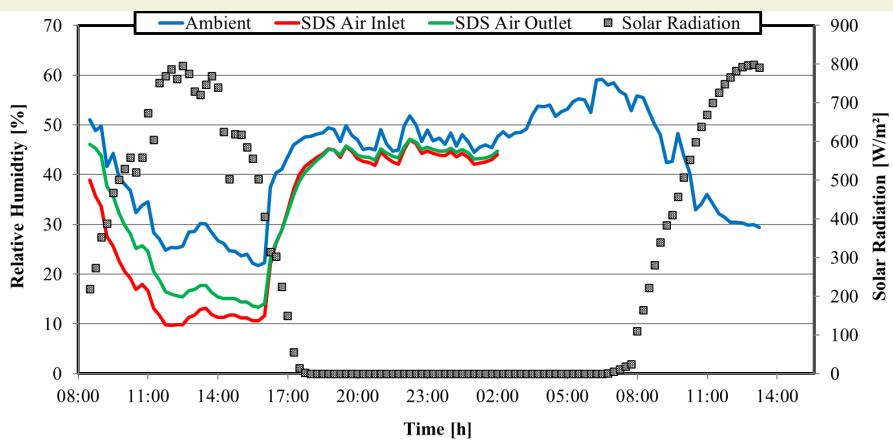

Figure 5. Variations of relative humidity and radiation during the drying of mushroom
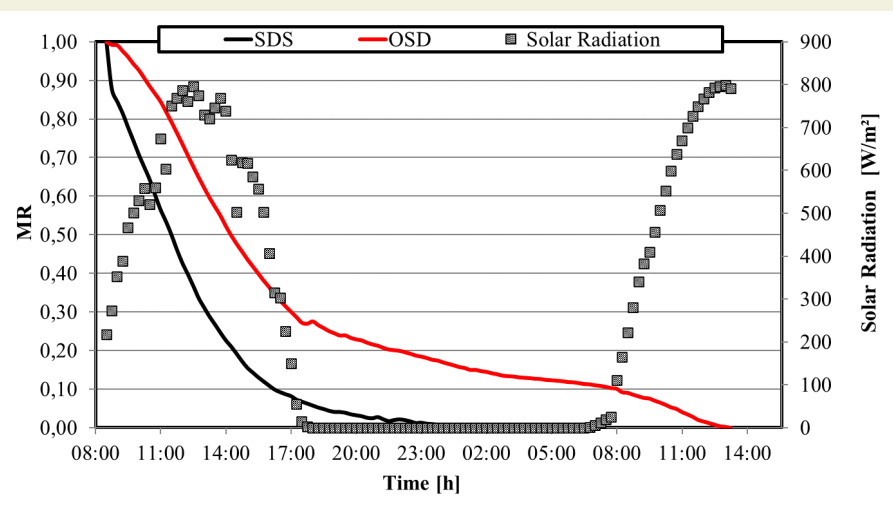

Figure 6. MR values of the dried mushrooms and solar radiation according to drying time in SD and OSD.

recorded.

Figure 4 represents the fluctuation in temperature and solar radiation recorded in the two drying procedures over the two-day continuous experiment with drying time. It was seen that the temperature values of different points varied depending on the radiation. Air at the inlet of the system (State 1-Ambient) gets warmed up in the collec-

tor (State 2-SD Air Inlet) and leaves the drying chamber (State 3-SD Air Outlet) at a temperature above the ambient temperature by taking the moisture from the product. During the drying process, the maximum temperatures within the drying chamber and outside were measured to be 44.48°C and 28.65°C, respectively, at sun radiation of 798.38 W/m². The temperature of the drying air and

the ambient air increased until noon, and the temperature values decreased with zero radiation in the evening during the drying process. The maximum temperature values of the products in the open sun drying and the drying chamber were recorded as 30.77°C and 29.67°C, respectively. The results were shown that the dried products in SD were at higher temperatures throughout the drying process than the dried products in OSD. Especially due to the adverse weather conditions during the night, the product dried with OSD has decreased to low-temperature values compared with product dried with SD. Figure 5 shows the variation in relative humidity and radiation over the course of the two-day experiment as measured at various sites on the system. It was noticed that the highest results were found for the relative humidity values at the solar collector and the chamber inlet at 59% and 44%, respectively.

Figure 6 shows variation of the MR values obtained for SD and OSD and the radiation with drying time. The moisture loss in the product during the daylight hours was higher than during the evening hours because of the radiation effect for both SD and OSD. While the drying process was completed on the first day in SD, the drying process was completed at the end of the second day in OSD. It was observed that the varies in the MR of the product for OSD were affected more by the weather conditions especially during the night. In addition, considering the drying time, the drying process with SD has been determined to reach the equilibrium moisture content

before drying with OSD (almost 12 hours early). This instance demonstrates the benefit of the SD system over the OSD approach. For SD and OSD, Figure 7 represents the change in drying rates (DR) of the mushroom with respect to MR through the drying process. In both plots, the first day drying rate was seen to be at its maximum value. It was presented that the DR curve of dried products in SD (Figure 7-a) showed a more regular change compared to the DR curve of the dried products in OSD (Figure 7-b). Figure 8 shows the picture of mushroom samples before and after drying in the SD. It is seen that the mushrooms dry and shrink through the drying process.

In this study, the experimentally obtained MR value for mushroom dried by both SD and OSD was estimated by 6 different thin-layer drying models and 6 different machine learning models. 6 thin-layer drying model constants, R, RMSE values are presented in Table 4 for MR experimentally obtained by SD. The best prediction among the nonlinear mathematical models was obtained by the Sripinyowanich and Noomhorn (Model No: 4) mathematical model since the model has the highest R (0.9998) and lowest RMSE (0.0051) rather than others.
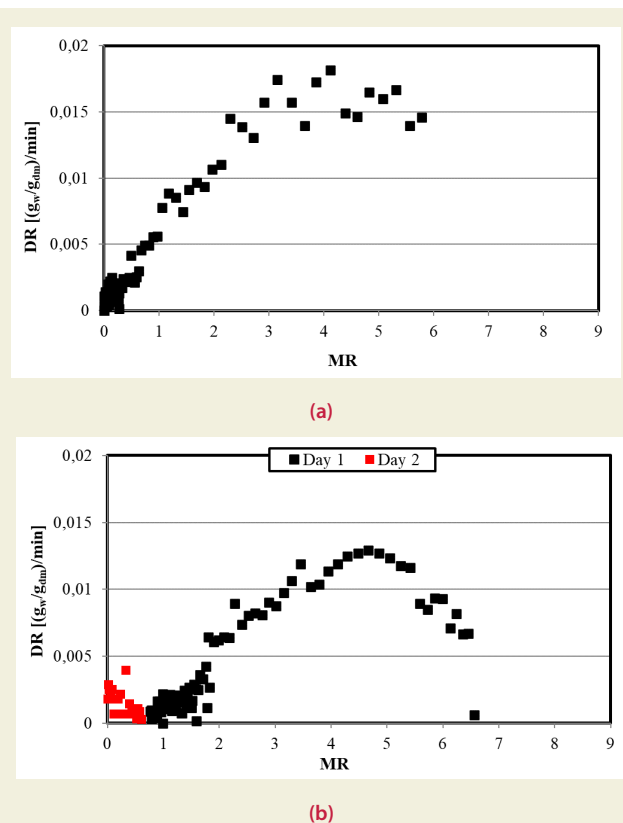

(a)

(b)

Figure 7. Variation of DR with MR values of mushroom dried with (a) SD and (b) OSD
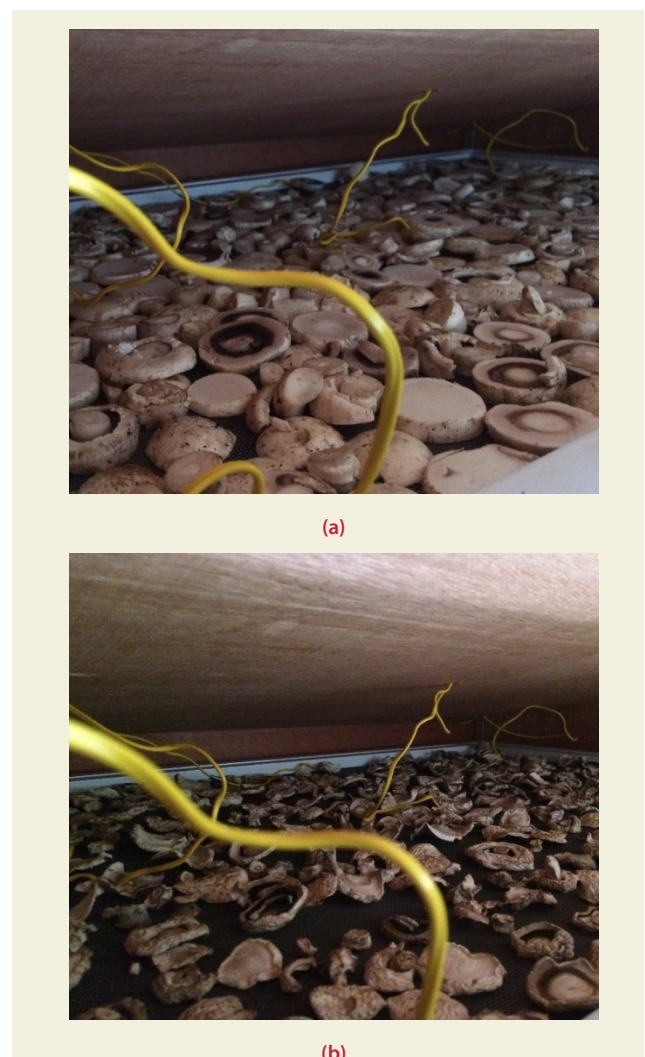

(a)

(b)

Figure 8. Picture of the mushroom slices before (a) and after (b) drying in the SD.

Table 4. Results from model studies for experimental MR obtained by drying mushrooms in SD

Model No	Model Constants	R	RMSE
1	a= 0.8967, k0= 2.463E-06, n= 1.337, b= 0.1033, k1= 0.08	0.9997	0.0061
2	a= -0.00886, b= 3.915, c= -1.25E+04, k= 8.455E-05	0.9996	0.0067
3	k= 7.3E-05, b=-2.955E-07	0.9967	0.0220
4	k=8.015E-06, n=1.216, b=1.064E-06, c=-0.05533	0.9998	0.0051
5	a=1.087, b= -0.07321, k0=7.634E-05, k1= 0.08, c=-0.01356	0.9992	0.0105
6	a=0.4896, b=1.001, k= 7.608E-5	0.9953	0.0265

Table 5. Statistical error rates obtained by estimating experimental MR values in mushroom drying with SD by different machine learning methods

Machine Learning Model	R	RMSE
MR_{M5P}	0.9864	0.0485
MR_{RF}	0.9899	0.0431
MR_{RT}	0.9898	0.0397
MR_{SVM}	0.9791	0.0569
MR_{SVM-II}	0.9781	0.0603
MR_{MLP}	0.9959	0.0252

The R and RMSE values were calculated by estimating the MR values of the mushrooms dried by SD with 6 different machine learning algorithms and predictive results of these models were presented in Table 5. The best estimate of the different machine learning was obtained with the Multilayer Perception (R=0.9959, RMSE = 0.0252).

In Table 6, 6 thin-layer drying model constants, R and RMSE values are given for OSD. The best prediction among the nonlinear mathematical models was obtained by the Hii et al. (Model No: 1) mathematical model since the model has the highest R (0.9975) and lowest RMSE (0.0197) rather than others. Table 7 shows R and RMSE results found by estimation of MR values of mushrooms dried by OSD with 6 different machine learning algorithms. The best estimate of the different machine learning was obtained with the Multilayer Perception Model (R=0,9998, RMSE=0.0122).

In Figures 9 and 10, the MR values are estimated by (a) MR_{M5P}, (b) MR_{MLP}, (c) $MR_{SVM-Poly}$, (d) $MR_{SVM-NPoly}$, (e) MR_{RT} and (f) MR_{RF} models were compared with exper-

imental MR values for SD and OSD methods, respectively. It was observed that the estimates obtained with the Random Forest Model were almost the same with the experimental data. This shows that the method that best predicts MR values is the Random Forest method (MR_{RF}). Since the MR parameter in the OSD shows more fluctuation, the MR parameter obtained in the OSD is more difficult to predict via regression models. In addition, it was seen that the performance parameters obtained from the mathematical models developed for SD gave better results than the performance parameters of the mathematical models developed for OSD. However, the MR parameter obtained in OSD was estimated with higher accuracy by machine learning algorithms compared to the MR parameter obtained in SD. The drying process with OSD was completed later than the drying process with SD (approximately 12 hours). Therefore, the number of experimental data obtained for MR in OSD is greater than the number of data obtained for MR in SD. The more data in machine learning models, the more accurate predictions are performed. This explains why the performance parameters of the machine learning models obtained for MR in OSD are higher than the machine learning models obtained for MR in SD.

4. Conclusions

The drying behaviours of the mushroom were investigated during two days of tests in the province of Osmaniye's environment using solar aided drying systems (SD) and open sun drying (OSD). Additionally, six distinct mathematical models and six different computer methods were applied for evaluating the moisture ratio for the dried mushrooms. The remarkable results are as follows.

Table 6. Results from model studies for experimental MR obtained by drying mushrooms in OSD

| Model No	Model Constants	R	RMSE
1	a=0.6878, k0=1.344E-07, n=1.596, b= 0.302, k1=1.786E-08	0.9975	0.0197
2	a=0.06871, b=2.257, c=-4099, k=5.653E-05	0.9937	0.0314
3	k=3.337E-05, b=1.484E-07	0.9889	0.0414
4	k=8.2000E-06, n= 1.3500, b= 1.0400e-06, c= -0.0800	0.9941	0.0302
5	a=1.081, b=-0.1272, k0=4.144E-05, k1=0.07, c= 0.04598	0.9939	0.0311
6	a=0.9931, b= -0.2303, k= 3.35E-05	0.9889	0.0415

- The total drying time obtained with SD was significantly reduced compared to the drying time obtained with OSD.

- The change in the MR values obtained with SD showed a smoother trend compared to the MR values obtained with OSD. The Sripinyowanich & Noomhorn model and Hii et al. model proved to become the best estimated non-linear mathematical models for the MR values obtained with SD and ODS, respectively.

- Among the machine learning algorithms, MR values of mushroom slices dried with SD and OSD were the best converging model of the Multilayer Perception (MLP) algorithm.

- In both drying methods, it was concluded that the MR found by the machine learning algorithms is

Table 7. Statistical error rates obtained by estimating experimental MR values in mushroom drying with OSD by different machine learning Methods

Machine Learning Model	R	RMSE
MR_{M5P}	0.9939	0.0364
MR_{RF}	0.9985	0.0191
MR_{RT}	0.9982	0.0194
MR_{SVM}	0.9894	0.0447
MR_{SVM-II}	0.9848	0.0502
MR_{MLP}	0.9998	0.0122
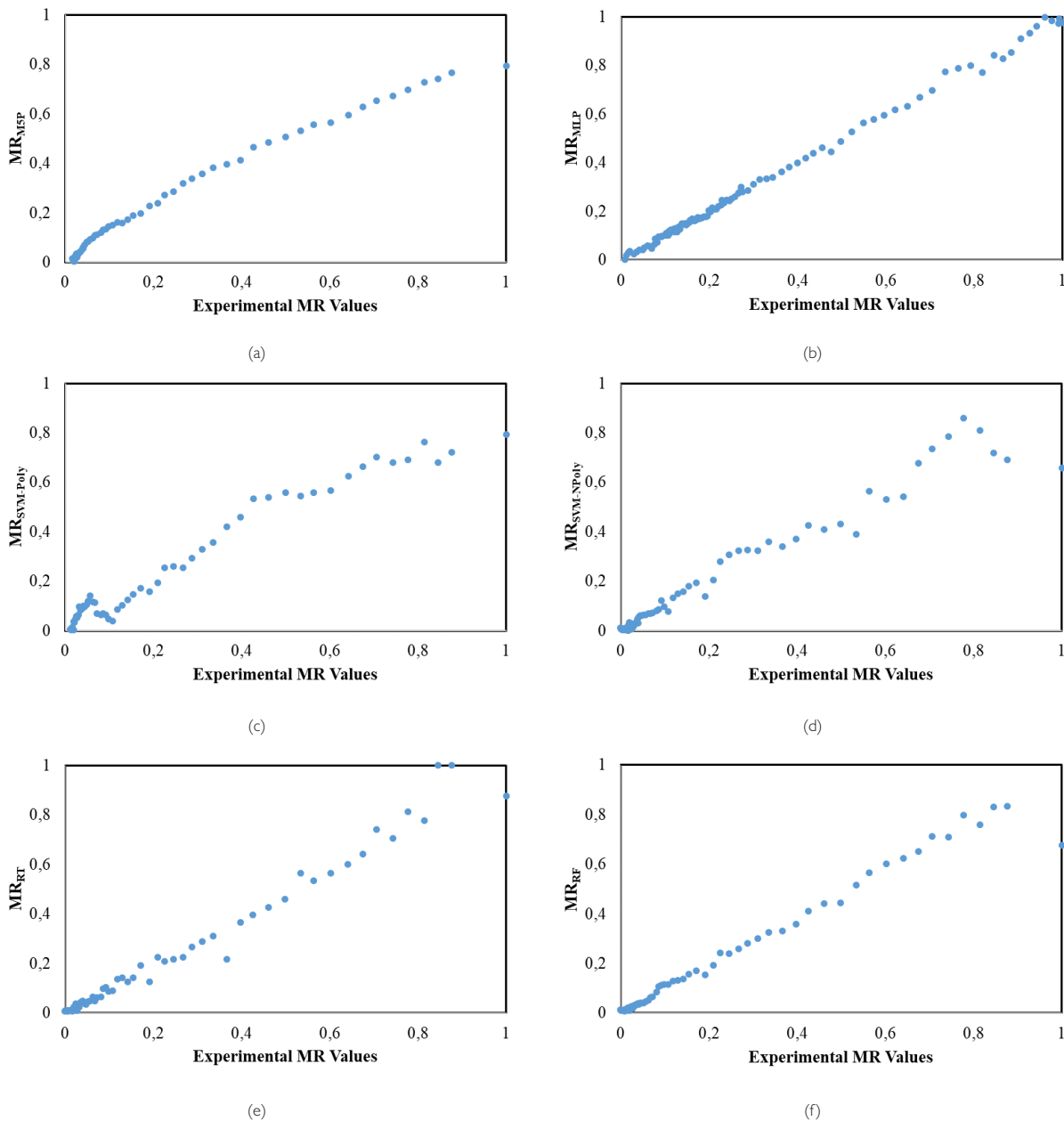
Figure 9. Comparison of (a) MR_{M5P}, (b) MR_{MLP}, (c) $MR_{SVM-Poly}$, (d) $MR_{SVM-NPoly}$, (e) MR_{RT} and (f) MR_{RF} with experimental data obtained in SD.
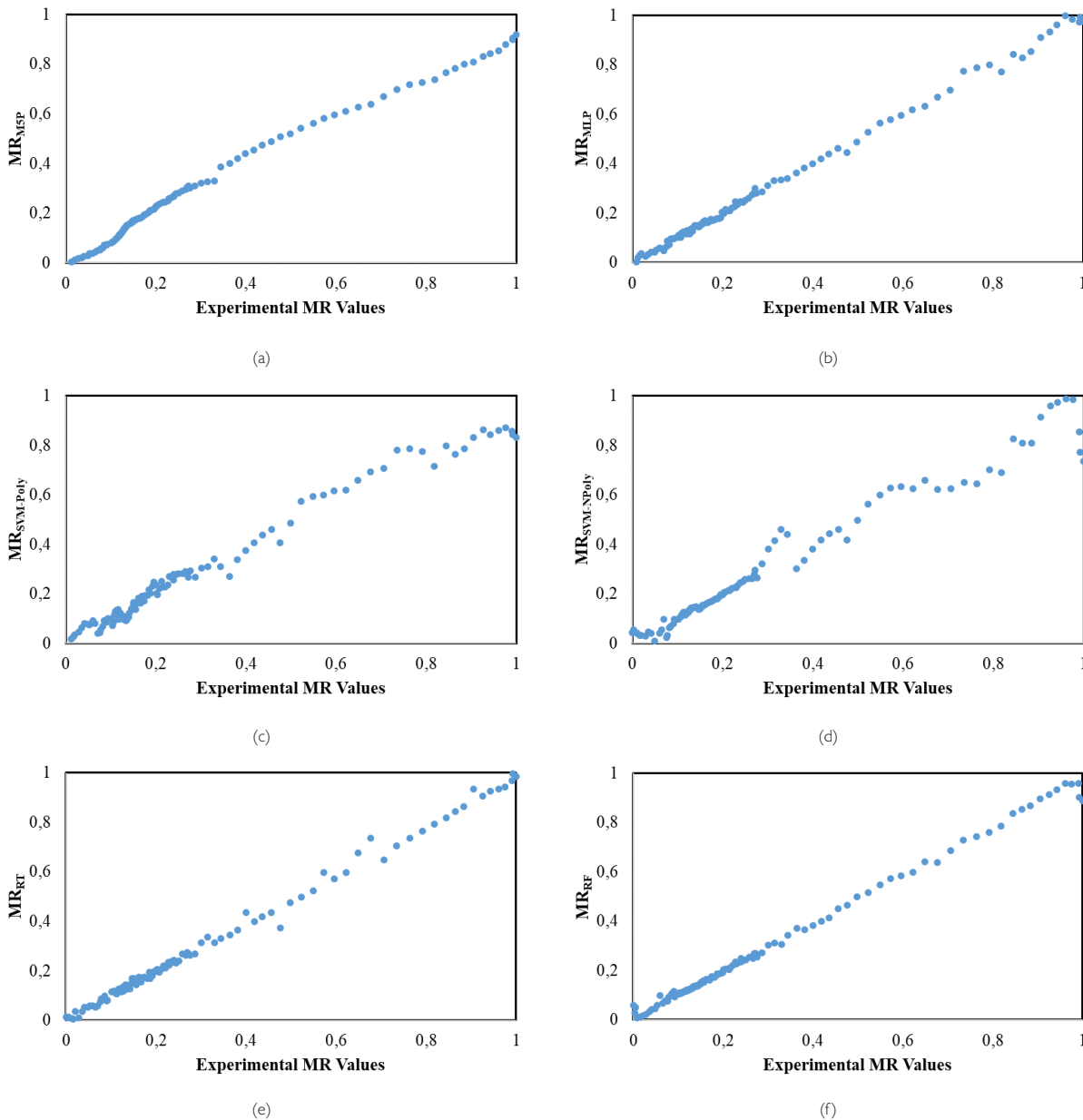
Figure 10. Comparison of (a) MR$_{M5P}$, (b) MR$_{MLP}$, (c) MR$_{SVM-Poly}$, (d) MR$_{SVM-NPoly}$, (e) MR$_{RT}$ and (f) MR$_{RF}$ with experimental data obtained in OSD.

better matched with the actual data according to the mathematically obtained MR values.

- It has been stated that using machine learning algorithms for more accurate modeling of MR in drying applications will yield better results.

5. Acknowledgements

6. References

[1]   Argyropoulos, D., Heindl, A., Müller, J. (2011). Assessment of convection, hot-air combined with micro-wavevacuum and freeze-drying methods for mushrooms with regard to product quality. International Journal of Food Science and Technology, 333–342, https://doi.org/10.1111/j.1365-2621.2010.02500.x.

[2]   Boroze, T., Desmorieux, H., Méot, J. M., Marouzé, C., Azouma, Y., Napo, K. (2014). Inventory and comparative characteristics of dryers used in the sub-Saharan zone: Criteria influencing dryer choice. Renewable and Sustainable Energy Reviews, 40, 1240-1259, https://doi.org/10.1016/j.rser.2014.07.058.

[3]   Moses, J., Norton, T., Alagusundaram, K., Tiwari, B. (2014). Novel Drying Techniques for the Food Industry. Food Enginering Review, 43-55, DOI 10.1007/s12393-014-9078-7.

[4]   Hnin, K. K., Zhang, M., Mujumdar, A. S., Zhu, Y. (2018). Emerging food drying technologies with energy-saving characteristics: A review. Drying Technology, 1465-1480,

https://doi.org/10.1080/07373937.2018.1510417.

[5] Uthpala, T. G. G., Navaratne, S. B., Thibbotuwawa, A. (2020). Review on low-temperature heat pump drying applications in food industry: Cooling with dehumidification drying method. Journal of Food Process Engineering, 43(10), e13502, https://doi.org/10.1111/jfpe.13502.

[6] Duan, X., Yang, X., Ren, G., Pang, Y., Liu, L., Liu, Y. (2016). Technical aspects in freeze-drying of foods. Drying Technology, 34(11), 1271-1285, https://doi.org/10.1080/07373937.2015.1099545.

[7] Mustayen, A., Mekhilef, S., Saidur, R. (2014). Performance study of different solar dryers: A review. Renewable and Sustainable Energy Reviews , 463–470, https://doi.org/10.1016/j.rser.2014.03.020.

[8] Tiwari, S., & Tiwari, G. N. (2016). Exergoeconomic analysis of photovoltaic-thermal (PVT) mixed mode greenhouse solar dryer. Energy, 114, 155-164, https://doi.org/10.1016/j.energy.2016.07.132.

[9] VijayaVenkataRaman, S., Iniyan, S., & Goic, R. (2012). A review of solar drying technologies. Renewable and sustainable energy reviews, 16(5), 2652-2670, https://doi.org/10.1016/j.rser.2012.01.007.

[10] Stritih, U., Osterman, E., Evliya, H., Butala, V., Paksoy, H. (2013). Exploiting solar energy potential through thermal energy storage in Slovenia and Turkey. Renewable and Sustainable Energy Reviews, 442–461, https://doi.org/10.1016/j.rser.2013.04.020.

[11] Mugi, V. R., Das, P., Balijepalli, R., & Chandramohan, V. P. (2022). A review of natural energy storage materials used in solar dryers for food drying applications. Journal of Energy Storage, 49, 104198, https://doi.org/10.1016/j.est.2022.104198.

[12] Olmuş, U., Güzelel, Y. E., Pınar, E., Özbek, A., Büyükalaca, O. (2022). Performance assessment of a desiccant air-conditioning system combined with dew-point indirect evaporative cooler and PV/T. Solar Energy, 231, 566-577, https://doi.org/10.1016/j.solener.2021.12.004.

[13] Kutlu, C., Erdinc, M. T., Li, J., Wang, Y., Su, Y. (2019). A study on heat storage sizing and flow control for a domestic scale solar-powered organic Rankine cycle-vapour compression refrigeration system. Renewable Energy, 143, 301-312, https://doi.org/10.1016/j.renene.2019.05.017.

[14] Srinivasan, G., Muthukumar, P. (2021). A review on solar greenhouse dryer: Design, thermal modelling, energy, economic and environmental aspects. Solar Energy, 229, 3-21, https://doi.org/10.1016/j.solener.2021.04.058.

[15] Wang, H., Zhang, M., Mujumdar, A. S. (2014). Comparison of Three New Drying Methods for Drying Characteristics and Quality of Shiitake Mushroom (Lentinus edodes). Drying Technology, 1791–1802, https://doi.org/10.1080/07373937.2014.947426.

[16] Fudholi, A., Sopian, K. (2019). A review of solar air flat plate collector for drying application. Renewable and Sustainable Energy Reviews , 333–345, https://doi.org/10.1016/j.rser.2018.12.032.

[17] Aktaş, M., Şevik, S., Özdemir, M. B., Gönen, E., (2015). Performance analysis and modeling of a closed-loop heat pump dryer for bay leaves using artificial neural network. Applied Thermal Engineering, 87, 714-723. http://dx.doi.org/ 10.1016/j.applthermaleng.2015.05.049.

[18] Doymaz, İ. (2011). Thin-layer drying characteristics of sweet potato slices and mathematical modelling. Heat Mass Transfer, 47, 277–285. http://dx.doi.org/ 10.1007/s00231-010-0722-3.

[19] Kooli. S., Fadhel. A., Farhat. A., Belghith. A. (2007). Drying of red pepper in open sun and greenhouse conditions Mathematical modeling and experimental validation. Journal of Food Engineering 79 (2007) 1094–1103, https://doi.org/10.1016/j.jfoodeng.2006.03.025.

[20] Chokphoemphuna, S., Chokphoemphunb A. (2018). Moisture content prediction of paddy drying in a fluidized-bed drier with a vortex flow generator using an artificial neural network. Applied Thermal Engineering, 145, 630–636. http://dx.doi.org/ 10.1016/j.applthermaleng.2018.09.087.

[21] Süfer, Ö., Sezer, S., Demir, H. (2017). Thin layer mathematical modeling of convective, vacuum and microwave drying of intact and brined onion slices. Journal Of Food Processıng and Preservatıon, 41, 1-13. http://dx.doi.org/10.1111/jfpp.13239.

[22] Çerçi, K., N., Süfer, Ö., Söyler , M., Hürdoğan , E., Özalp , C. (2018). Thın Layer Dryıng of Zucchını In Solar Dryer Located In Osmanıye Regıon, Tehnıčkı Glasnık, 12, 79-85, http://dx.doi.org/ 10.31803/tg-20180126094515.

[23] Akman, H. (2017). Thermodynamic Analysis of a Solar Energy Assisted Drying System, MSc Thesis (in Turkish) , Osmaniye Korkut Ata University, Osmaniye.

[24] Hürdoğan, E., Çerçi, K. N., Saydam, D. B., Ozalp, C. (2022). Experimental and modeling study of peanut drying in a solar dryer with a novel type of a drying chamber. Energy Sources, Part A: Recovery, Utilization, and Environmental Effects, 44(2), 5586-5609, https://doi.org/10.1080/15567036.2021.1974126.

[25] Holman JP. (2001). Experimental methods for engineers. 8th ed. McGraw Hill.

[26] Kavak Akpinar, E., Toraman, S., (2016). Determination of drying kinetics and convective heat transfer coefficients of ginger slices. Heat Mass Transfer, 52, 2271–2281. http://dx.doi.org/ 10.1007/s00231-015-1729-6.

[27] Hii, C. L., Law, C. L., Cloke, W. (2009). Modeling using a new thin layer drying model and product quality of cocoa. Journal of Food Engineering, 90, 191-198. https://doi.org/10.1016/j.jfoodeng.2008.06.022.

[28] Figiel, A. (2009). Drying kinetics and quality of vacuum-microwave dehydrated garlic cloves and slices. Journal of Food Engineering, 94, 98-104. https://doi.org/10.1016/j.jfoodeng.2009.03.007.

[29] Erbay, Z. Icier, F., (2010). A review of thin-layer drying of foods: theory, modeling, and experimental results. Critical Reviews in Food Science and Nutrition, 50, 441-464. https://doi.org/10.1080/10408390802437063.

[30] Sripinyowanich, J. Noomhorm, A. (2011). A new model and quality of unfrozen and frozen cooked rice dried in a microwave vibro-fluidized bed dryer. Drying Technology, 29, 735-748. https://doi.org/10.1080/07373937.2010.535399.

[31] Noomhorn, A. Verma, L. R. (1986). Generalized single-layer rice drying models. Transactions of the ASAE, 29, 587-591. https://doi.org/10.13031/2013.30194.

[32] Yaldız, O., Ertekin, C., (2001). Thin layer solar drying of some vegetables. Drying Technology, 19, 583–596. http://dx.doi.org/ 10.1081/DRT-100103936.

[33] Sun, Y., Zhang, M., Mujumdar, A. S., & Yu, D. (2021). Pulse-spouted microwave freeze drying of raspberry: Control of moisture using ANN model aided by LF-NMR. Journal of Food Engineering, 292, 110354, https://doi.org/10.1016/j.jfoodeng.2020.110354.

[34] Şanlitürk, E. (2018). Prediction of Defective Product with Machine Learning Algorithms, MSc Thesis (in Turkish) Istanbul: Istanbul Teknik University.

[35] Ayhan, S., Erdoğmuş, Ş. (2014). Kernel Function Selection for the Solution of Classification Problems via Support Vector Machines. Eskişehir Osmangazi University Journal of Economics and Administrative Sciences, 9(1), 175-201.

[36] Deka, P. C. (2014). Support vector machine applications in the field of hydrology: a review. Applied soft computing, 19, 372-386, https://doi.org/10.1016/j.asoc.2014.02.002.

[37] Henderson, S. M. Pabis, S. (1961). Grain drying theory I: temperature effect on drying coefficient. Journal of Agricultural Engineering Research, 6, 169-74.

[38] Karimipour, A., Bagherzadeh, S., A., Taghipour, A., Abdollahi, A., Safae, M., R. (2019). A novel nonlinear regression model of SVR as a substitute for ANN to predict conductivity of MWCNT-CuO/water hybrid nanofluid based on empirical data. Physica A, 521, 89-97. https://doi.org/10.1016/j.physa.2019.01.055.

[39] Das, M., Akpinar, E., K. (2018). Investigation of Pear Drying Performance by Different Methods and Regression of Convective Heat Transfer Coefficient with Support Vector Machine. Applied Science, 8, 215. doi:10.3390/app8020215.

[40] Sattari, M. T., Feizi, H., Colak, M. S., Ozturk, A., Apaydin, H., Ozturk, F. (2020). Estimation of sodium adsorption ratio in a river with kernel-based and decision-tree models. Environmental Monitoring and Assessment, 192(9), 1-13, https://doi.org/10.1007/s10661-020-08506-9.

[41] Quinlan, J. R. (2014). C4. 5: programs for machine learning. Elsevier.

[42] Zhan, C., Gan, A., Hadi, M. (2011). Prediction of lane clearance time of freeway incidents using the M5P tree algorithm. IEEE Transactions on Intelligent Transportation Systems, 12(4), 1549-1557, Doi: 10.1109/TITS.2011.2161634.

[43] Güzelel, Y. E., Olmuş, U., Çerçi, K. N., Büyükalaca, O. (2021). Comprehensive modelling of rotary desiccant wheel with different multiple regression and machine learning methods for balanced flow. Applied Thermal Engineering, 199, 117544, https://doi.org/10.1016/j.applthermaleng.2021.117544.

[44] Behnood, A., Behnood, V., Gharehveran, M. M., Alyamac, K. E. (2017). Prediction of the compressive strength of normal and high-performance concretes using M5P model tree algorithm. Construction and Building Materials, 142, 199-207, https://doi.org/10.1016/j.conbuildmat.2017.03.061.

[45] Akman, M. (2010). An overview of data mining techniques and analysis of Random Forests method: An application on medical field, MSc Thesis (in Turkish), Ankara University, Ankara.

[46] Messikha,N., Bousbaa, S., Bougdaha N. (2017). The use of a multilayer perceptron (MLP) for modelling the phenol removal by emulsion liquid membrane. Journal of Environmental Chemical Engineering. 5, 3483–3489. http://dx.doi.org/10.1016/j.jece.2017.06.053.